Numerical Analysis and Theoretical Modeling of Causal Effects of Conscious Intention

DR. RICHARD L. THOMPSON

Bhaktivedanta Institute
1136 Grand Ave., San Diego, CA 92109

In this paper we discuss some phenomena involving interactions between machines and states of conscious intention that have been reported by Robert Jahn and his colleagues at Princeton University. We specifically deal with the experiments carried out by these investigators with an apparatus called the random mechanical cascade (or RMC). We introduce a class of theories, called selection theories, which might be invoked to explain the phenomena they have observed. These include some parapsychological theories that have been proposed for such phenomena in the past, and they also include the theory that the phenomena are spurious by-products of conscious or unconscious editing of the experimental data.

We have found that the data for the RMC experiments have some statistically significant features which have not been noted before, and which tend to rule out selection theories as possible explanations of the observed phenomena. We also show by an analysis of the RMC apparatus that these phenomena cannot be readily explained as due to the application of external forces to the apparatus. Thus our findings support the conclusion that these phenomena represent a genuine anomaly, and they narrow down the range of possible theories that might account for this anomaly.

INTRODUCTION

A group at Princeton University including R. G. Jahn, B. J. Dunne, and R. D. Nelson has for several years carried out a research program investigating correlations between human intentions and the behavior of various machines. In one series of experiments the machine was a version of a device commonly used to demonstrate the law of large numbers. The Princeton device, called a "Random Mechanical Cascade" or RMC, was described as follows in Nelson, Dunne, and Jahn (1988a and 1988b): The machine consists of a quincunx array of 330 3/4" nylon pins with a horizontal spacing of 3.25". A total of 9000 3/4" polystyrene spheres are allowed to cascade through the array from an inlet at the top, and these accumulate in 19 equally spaced collecting bins at the bottom. About 12 minutes are required for all of the balls to reach the bins.

As one would expect, the 9000 balls tend to fill the bins according a Gaussian distribution, but this distribution is somewhat irregular, and its mean and other statistical features tend to vary randomly. In the Princeton experiments an observer, called an "operator", would try to influence the mean of the distribution to shift to the left, remain at the baseline (the statistically expected position), or shift to the right. The operator did this by meditation within the mind, rather than by trying to physically interfere with the machine. Usually the operator sat in front of the machine at a distance of about eight feet and watched the cascading balls, but in some experiments the operator was at a remote location.

The operation of the machine was divided into sets of three "tripolar" runs, one for each of the three intentions of left, baseline, or right. (In some cases the operator was free to choose the order of the intentions in each set, and in other cases this was dictated by the experimental protocol.) An operator would perform a number of series, each consisting of 10 or 20 tripolar sets. The distribution of the balls in the bins was counted electronically for each run and recorded automatically in a computer file.

The performance of the operators was evaluated by examining the behavior of the quantities LT-BL, RT-BL, and RT-LT, where LT, BL, and RT are the cumulative bin distribution means for the intentions, left, baseline, and right, over a long series of runs. Differences between LT, BL, and RT were used to offset the effect of long term trends in machine behavior caused by wear and other systematic factors. We note that since there are 19 bins, the bin distribution mean for a perfectly symmetrical machine should come out to 10. Since the actual machine is slightly asymmetrical, this mean tends to be just over 10.

One would naturally expect that there would be no relationship between human states of consciousness and the statistical behavior of the machine. However, the experiments indicated that in the long run, this behavior tended to conform with the intentions of the operators. In a total of 1131 tripolar sets of runs generated by 25 operators, it was found that the cumulative RT-LT came out to about 6.45. This corresponds to an average mean for rightward intentions of 10.0229 and an average mean for leftward intentions of 10.0172. Although the differences between these means are quite small, they turn out to be statistically significant. The standard deviation for RT-LT was .0493, and the corresponding Student t-score was 3.891. This outcome has a probability of about 5×10^{-5}, if we assume that the individual runs were statistically independent and not influenced by operator intention.

In these experiments the bulk of the runs were generated by two operators (10 and 55), and operator 10 achieved by far the most significant results. However, a statistically significant effect remains, even if the data generated by operators 10 and 55 are excluded from the analysis.

In this paper we will analyze the results of the random mechanical cascade experiments, and show that the data generated by these experiments reveals some anomalous effects in addition to those originally reported. To do this, it was necessary for us to gain access to the original RMC data, and this was kindly provided by Roger Nelson of the engineering anomalies research group at Princeton. In Section 1 we discuss the physics of the RMC, and we show why it would be difficult to produce the observed anomalous effects by physically influencing the machine. In Section 2 we introduce the class of selection theories and give three examples of such theories. In Section 3 we discuss the RMC data, and we show how it reveals hitherto unknown anomalous effects that should not occur, according to selection theories. Finally, in Section 4 we summarize our conclusions.

1. THE EFFECT OF SMALL FORCES ON THE RMC

What happens when a conscious person desires to perform some action, such as picking up an object? Standard explanations maintain that the desire to act can be identified with particular electro-chemical phenomena in neurons within the brain. These give rise to

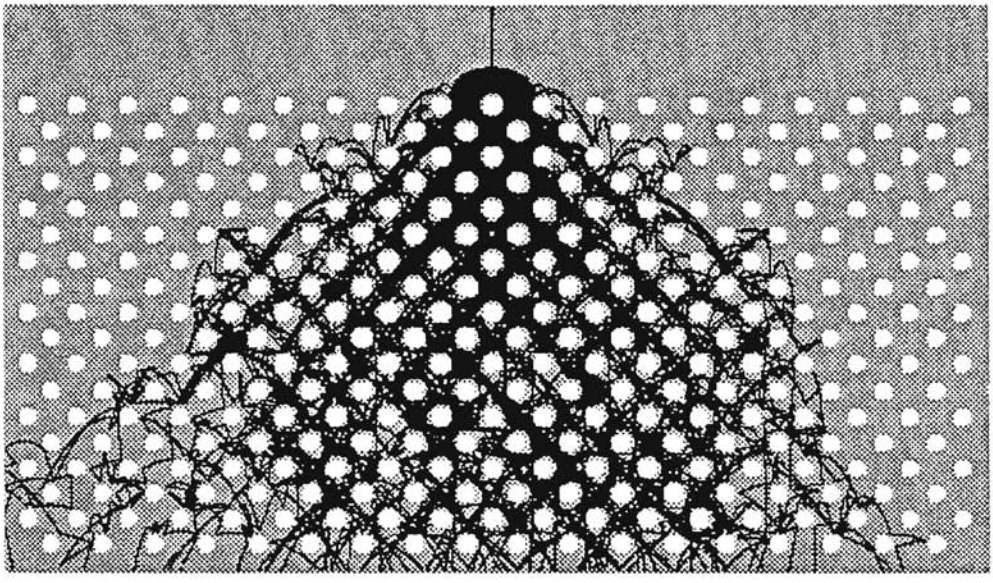

Figure 1(a). Random mechanical cascade model, 100 trajectories.

movements of bodily parts and possible changes in the body's electrical field and other physical characteristics. Could these changes in turn influence the behavior of the RMC in a normal physical fashion?

Nelson *et. al.* (1988a, pp. 33–34) discuss possible mechanical, electromagnetic, and gravitational interactions between the observer and the RMC, and reject these as being too weak by several orders of magnitude to produce the observed effects. However, our analysis shows that this is not correct. As we will show, extremely small forces can significantly affect the behavior of the RMC.

This might seem to imply that the observer could systematically influence the machine by generating such small forces by ordinary means. But this is also not correct, since extremely small changes in the applied forces will have large, unpredictable affects on the RMC. If the observed anomalous behavior of the RMC is due to small forces generated in a normal way as a result of conscious intention, then these forces must be applied with great precision at properly selected magnitudes (and it is also necessary to compensate for the effects of many other small forces originating in the general environment of the machine). Thus the observed anomaly involves either a completely unknown type of interaction between intention and machine behavior, or it involves known physical forces controlled in an unknown way with inexplicable precision.

To study the influence of small forces on the RMC, we devised an idealized, two dimensional RMC model. Using this model, we can consider what would happen if a uniform horizontal acceleration, h, were applied to each ball during the time of its descent through the RMC. We can think of this acceleration as being due to the gravitational attraction of a mass situated outside of the machine.

Figure 1(a) illustrates the paths followed by 100 balls through this model. The "balls" are actually points that bounce from an array of disks 1.5" in diameter with a horizontal

TABLE 1

The Effect of Uniform Horizontal Acceleration on a Random Mechanical Cascade Model

	Accelera-tion (cm/sec^2)	Bin Mean (bins)	X-axis Mean (cm)		Accelera-tion (cm/sec^2)	Bin Mean (bins)	X-axis Mean (cm)
1	.000000	10.02	.21730	18	400000	9.90	-.53943
2	.000001	10.47	3.80527	19	.400010	9.75	-2.18546
3	.000002	9.45	-4.55733	20	.500000	10.06	.99440
4	.000003	9.67	-2.84750	21	.500010	10.02	.30825
5	.000004	10.08	.43019	22	.600000	10.18	1.68766
6	.000005	9.55	-3.73401	23	.600010	9.97	-.24389
7	.000006	9.60	-3.21256	24	.700000	10.44	3.59713
8	.000007	9.92	-.52338	25	.700010	10.08	.59416
9	.000008	9.32	-5.32070	26	.800000	9.97	-.37369
10	.000009	9.84	-1.57568	27	.800010	10.09	.67769
11	.000010	9.96	-.39112	28	.900000	9.84	-.98738
12	.100000	9.76	-2.07684	29	.900010	10.06	.46973
13	.100010	9.82	-1.46087	30	1.000000	10.17	1.18056
14	.200000	10.52	4.46410	31	1.000010	9.58	-3.48291
15	.200010	10.37	2.81123				
16	.300000	10.49	4.48820				
17	.300010	9.72	-2.44460				

Here the x-axis mean is the average x value of 100 points reaching the x-axis at the bottom the diagram in Figure 1(a). This axis is divided into 19 3.25" bins with bin 10 centered at x=0, and the bin mean is computed from the histogram for points entering these bins. (In these computations the initial angles of motion of the incoming points ranged from -5 to +5 degrees.)

spacing of 3.25"; since we do not allow the "balls" to spin, this is mathematically equivalent to having .75" diameter disks bouncing from .75" diameter disks. The points also bounce from vertical walls marked by the edge of the gray region in the figure, but they do not interact with one another. The points bounce elastically, losing a certain percentage of their velocity on each bounce, and they move parabolically according to the acceleration of gravity between bounces. The moving points enter from a point directly above one of the fixed disks. Their initial velocities are fixed in magnitude and are directed at evenly spaced angles, a, from the vertical.

Table 1 shows what happens in this model if we add a small, uniform horizontal acceleration, h, to the motion of the points. In the absence of fixed disks to bounce from, one would expect such an acceleration to shift the x-axis mean by hD/g, where D is the

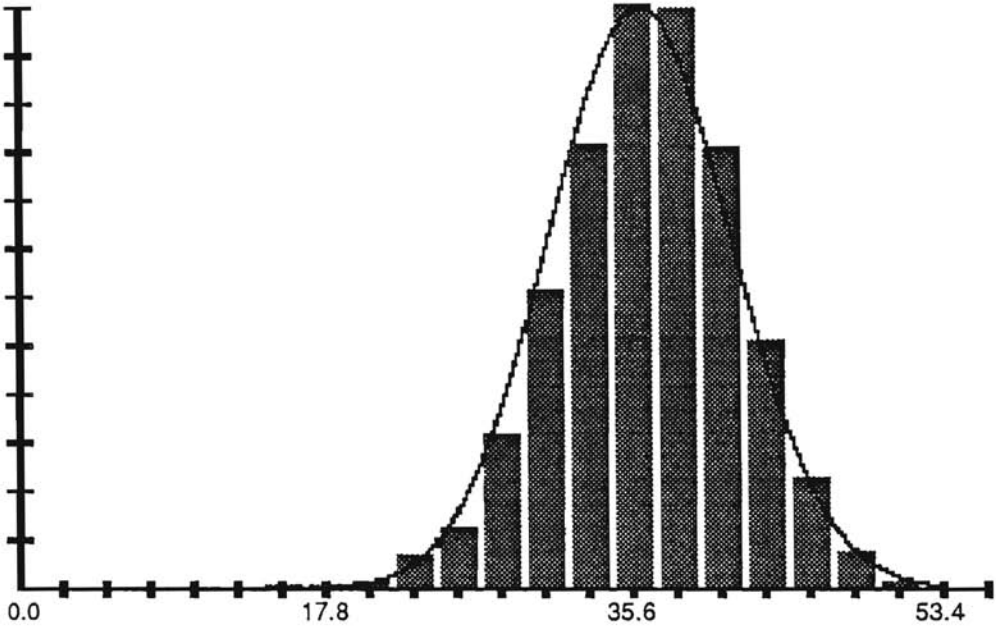

Figure 1(b). Histogram of $\log_{10}|dx/da|$, where x is the ball x-position on entering the bins and a is the initial angle of the ball at the start of its trajectory.

vertical distance from the inlet to the bins, and g is the acceleration of gravity. (Here D is 90 cm.) Such a shift should also occur in the presence of fixed disks, but the question is: Do the disks cause the acceleration to have a greater effect?

In Table 1 we can see that small accelerations can have a large effect on the x-axis and bin means, but this effect cannot be predicted either in terms of magnitude or direction. The reason for this is can be seen in the histogram in Figure 1(b). The position, x, of a point once it reaches the x-axis, is a function, x(a), of the point's initial angle of motion, a. The histogram in Figure 1(b) gives the distribution of |dx(a)/da| for 6000 points ranging in initial angle from -10^{-4} to $+10^{-4}$ degrees. We can see that for typical points, this derivative is as large as 10^{36}. Since x(a) remains within fixed limits, this means that this function must oscillate wildly as the angle a varies.

A 1 gram mass at a distance of 1000 km produces a gravitational acceleration of about 6.67×10^{-26} m/sec^2, and this will cause an object falling from rest to deviate from the vertical by about 6.8×10^{-27} radians. Thus, forces of this magnitude could strongly affect the motion of the balls in the RMC.

The large values of |dx(a)/da| are due to the fact that with each bounce of a point from a disk in our model, uncertainties in the direction of motion of the point are magnified by roughly a factor of 10. Thus |dx(a)/da| is roughly 10^n, where n is the number of bounces made by the point during its descent. This exponential amplification of small uncertainties is an example of the phenomenon of deterministic chaos, which is very common in nonlinear systems. In this case, the amplification of small effects is caused by elastic collisions between objects with curved surfaces. This phenomenon can be expected in the

TABLE 2

Average Bin and X-axis Means for Groups of Accelerations of the form .5+N10^{-6} for N ranging from N1 to N2 by DN

N1,N2,DN	Average Bin Mean	Average X-axis mean
-15,15,1	10.24	2.05466
16,46,1	10.11	.88560
47,77,1	10.13	1.06291
-150,150,10	10.07	.55741
-1500,1500,100	10.03	.25061

Compare with line 20 of Table 1.

real RMC, as well as in our two dimensional model.

Although we can expect extremely small forces to exert large influences on the motion of the balls, these influences will be unpredictable, and thus it would be practically impossible to influence the motion of the balls in a systematic way by imposing such forces on them. Only the average effects produced by randomly varying forces could be exploited to produce systematic effects. Although such average effects could be studied using our simplified model, we have not pursued this study due to the large amount of computer time it would require. Table 2 is a list of 5 examples of averages of 31 closely spaced accelerations that are close to .5 cm/sec^2. These averages suggest that there is a positive effect near h=.5, but averages sampling more points might give a different result.

We suspect that, on the average, fluctuations in imposed forces will tend to smooth out the wild oscillations shown in Table 2, and we therefore expect that the effects of these forces will be only a few orders of magnitude larger than the forces themselves. Thus, if we limit ourselves to the idea that the intentions of the operators somehow bring about forces that produce the observed experimental effects, then we are left with the following dilemma: Either these forces are relatively strong and are very hard to account for in terms of known physical principles, or they are extremely weak. In the latter case, if the forces vary somewhat at random, then they will have extremely weak net effects. Even if they remain very steady, it is still hard to see how an individual could adjust them with the extreme precision needed to produce desired results. And there is the problem that extremely weak forces from the general environment will also be influencing the RMC in an unpredictable way.

It has been pointed out that applying a horizontal force, h, is equivalent to rotating the RMC, and that a rotation of, say, 1 degree should definitely shift the bin mean in a predictable way. This is true, but such a rotation constitutes a very drastic

interference with the machine, and the corresponding force, h, is very large. This h is .017g, and it corresponds to the gravitational pull of about 25.7 million kg at a distance of 1 meter. In contrast, the intervals between the closely spaced accelerations in Table 2 and also in lines 1–11 of Table 1 are 10^{-6} cm/sec^2. We note that this is the acceleration produced by a 150 pound mass at about 67.4 cm. Thus if a person of average weight walked up to the RMC, the change in h would be about the size of the smallest increments used in Tables 1 and 2. (Of course, due to the size of the RMC, not all of the balls would be at 67.4 cm.) Our point is that forces of this magnitude produce strong but completely unpredictable effects on the bin mean.

2. SELECTION THEORIES

There is a class of theories, called selection theories, that might be invoked to explain the anomalous RMC findings. Such theories can be described in general terms as follows: Let us suppose that natural processes obeying known physical laws produce an ensemble of possible outcomes for runs of the RMC. This ensemble can be defined by a probability distribution, P(x), where x is the information representing an RMC run. Let y represent the observer's state of intention, and let f(x,y)>0 measure the degree to which a run x satisfies the intention y. (Here y=RT, LT, or BL.) We suppose that the greater the agreement between the run and the intention, the greater is f(x,y). Define the following probability distribution for a pair, (x,y), consisting of a run plus an intention:

$$P'(x,y) = f(x,y)P(x)/K \tag{1}$$

where K is a normalization constant. In a selection theory, the actual, measured probability distribution for (x,y) is given by P'(x,y), for some suitable function, f(x,y). We will give three examples of selection theories, and show in each case how one arrives at P'(x,y).

Example (1), precognition. The first example assumes that the RMC always behaves according to known physical laws, but that the observer has a paranormal ability to foresee the future. In this example we suppose that the observer has the opportunity to make his own choice of intentions prior to each run (the "volitional" mode). We suppose that he makes his choice in accordance with what he foresees, but that his foresight is imperfect. This can be expressed by means of a Markov chain transition matrix, M(x,y), which gives the probability that the observer will choose intention y, given that the future run will be x. In this model, the probability that (x,y) will come up is

$$P'(x,y) = P(x)M(x,y) \tag{2}$$

which has the same form as Eqn. (1). In the case where the intentions are chosen in advance by the experimenters (the "instructed" mode), a similar model can be formulated on the basis of precognition by the experimenters.

Example (2), wave function collapse. The extremely large values of |dx/da| discussed in the last section imply that during a run, the quantum mechanical wave function for the RMC

should spread out to encompass a range of outcomes for that run. Thus, the normal physical behavior of the RMC can be expressed in terms of the collapse of the quantum mechanical wave function. We can let Ψ represent a wave function of the RMC plus observer that encompasses many possible run outcomes, and let Φ_i represent wave functions of the RMC plus observer for specific outcomes. (Just to simplify the discussion, let us suppose that the Φ_i's form an orthonormal basis for wave functions.)

In quantum mechanics, the probability of getting state Φ_i after collapse of the wave function, Ψ, is $|\langle\Psi,\Phi_i\rangle|^2$. Wigner (1970) has argued that the collapse of the wave function is connected with consciousness, and he proposes that a proper formulation of this connection will require modifications of the laws of quantum mechanics. So, if we suppose that consciousness prefers Φ_i's showing harmony between intention and RMC run, we can venture to express this by replacing $|\langle\Psi,\Phi_i\rangle|^2$ by $f(\Phi_i)|\langle\Psi,\Phi_i\rangle|^2$, where f is a positive function that favors such harmony. This modified form of quantum mechanics is also a selection theory.

Example (3), data selection. In this theory we suppose that the observed correlation between intention and RMC behavior is spurious. The probability of run outcome x is determined by a distribution P(x), which is generated in accordance with the laws of physics. But in the natural course of events, some runs may seem defective for one reason or another, and the experimenter may wish to delete them from the database. We suppose that, owing to the desire for a successful experiment, the experimenter is more likely to throw out runs where x disagrees with the intention, y, than runs where x agrees. (He may do this consciously or subconsciously.) This can be expressed by means of a data selection function, $0<f(x,y)<1$, which represents the chances of retaining a particular run in the database, and which is somewhat smaller for cases where x and y disagree than it is for cases where they agree. The probability for (x,y) in the edited database is then given by Eqn. (1).

Let us suppose that the run information, x, can be expressed as x=(u,v,w), where u and v are real variables describing different features of the run, and w contains whatever additional information is needed to specify x. We can suppose that v is the variable to which intentions apply (namely, the bin mean in the RMC experiments). Since f(x,y) expresses the degree of agreement between v and the intention, y, we can write it as $f_1(v,y)$.

If we substitute x=(u,v,w) into Eqn. (1), and then eliminate the variable w by summing over it, we obtain an equation of the form

$$P'(u,v,y) = f_1(v,y)P(u,v)/K \tag{3}$$

The dependence of v on y in this model can be seen by examining the expected value of v, given y. This expectation value is

$$E(v|y) = \int \int vP'(u,v,y)dudv / \int \int P'(u,v,y)dudv \tag{4}$$

and we can similarly define E(u|y), the expected value of u, given y.

The model is designed so that E(v|y) varies as the intention, y, varies. But what does the model say about how the variable, u, varies as y varies? We can readily calculate this if we assume that the distribution, P(u,v), for u and v is a bivariate normal distribution with means, m_u, m_v, standard deviations, s_u, s_v, and correlation coefficient, r. Given this

assumption, we find that,

$$[E(u|y)-m_u]/s_u = r[E(v|y)-m_v]/s_v \quad (5)$$

The distribution, P(u,v), depends on the physics of the RMC. This equation tells us that if u and v are not strongly correlated in P(u,v), then E(u|y) will vary only weakly as the intention, y, is varied.

We will show in the next section that we can find an RMC variable, u, for which P(u,v) is approximated by a bivariate normal distribution with a small r, but for which E(u|y) does vary strongly with y, in violation of Eqn. (5). This implies that the RMC data cannot be realistically modeled by a selection theory, and in particular, it cannot be modeled by theories (1) through (3), above.

3. ANALYSIS OF THE DATA

The information describing an RMC run is given by 19 bin numbers, b(1), . . . ,b(19), indicating the number of balls that fall in each of the 19 bins. This sequence of 19 numbers is called the bin distribution for the run. The bin mean is simply the expected value of i for the distribution, b(i), i=1, . . . ,19. We wanted to find additional variables that (1) are functions of the 19 bin numbers, (2) are physically meaningful, and (3) are nearly statistically independent of the bin mean and of one another. Our objective in defining such variables was to find candidates for the u of Eqn. (5).

The distribution of balls in the bins can be approximated by a Gaussian. In Nelson *et. al.* (1988b), it is observed that the bin distribution tends to deviate from a Gaussian in the center due to the tendency of some balls to fall straight down for some distance without striking pins, and at the sides due to bouncing of the balls from the sides of the machine. The deviation in the center takes the form of a second, narrower Gaussian superimposed on the main bin distribution Gaussian. The bouncing of the balls from the sides contributes an additional U-shaped curve that is superimposed on these two Gaussians. Thus, the bin distribution can be broken down into the sum of these three curves, each of which can be explained in terms of the physics of the RMC.

Let Dist(1), . . . ,Dist(19) stand for the bin distribution for a given run. We tried to break down Dist into the three components just mentioned. The first of these is Gauss1, an approximation to Dist by a Gaussian. This was obtained by fitting a quadratic to log(Dist(3)), . . . ,log(Dist(7)),log(Dist(13)), . . . ,log(Dist(17)) by least squares, and expressing Gauss1 as the exponential of that quadratic. In the least squares fit, we avoided the bins in the middle and on the ends since for these bins, Dist tends to deviate from a Gaussian.

The next step is to scale Gauss1 so that its total, Gauss1(1)+ . . . +Gauss1(19), is maximal, given that

$$\text{Dist2}(i) = \text{Dist}(i) - \text{Gauss1}(i) \geq 0 \quad (6)$$

for i=1, . . . ,19. When we do this we find that Dist2 has the shape of a Gaussian, but is narrower than Gauss1. We therefore define the second component as Gauss2, a Gaussian

approximation to Dist2. This Gaussian is defined to have the same mean and standard deviation as Dist2 on bins 3–17 (avoiding the non-Gaussian behavior on the sides), and it is scaled so that its root-mean-square difference from Dist2 is minimal.

The total of Gauss1 cannot exceed 9000, the total number of balls per run, and it generally is about 7700. The total for Gauss2 is generally somewhat over 1000.

The third component, called Rem (for remnant), is defined by

$$\text{Rem}(i) = \text{Dist2}(i) - \text{Gauss2}(i) \tag{7}$$

for i=1,...,19. We note that Rem(i) may take on negative values.

Figure 2(a) illustrates the breakdown of Dist into Gauss1, Gauss2, and Rem in a particular case. It is interesting that Rem has a remarkably consistent form. Figure 2(b) shows the superposition of Rem curves obtained from 30 different bin distributions. The elevation at the sides is presumably due to reflection of balls from the side walls, and the other characteristics must be due to asymmetries in the structure of the machine.

For each run, we can compute a number of standard parameters for the distributions, Dist, Gauss1, and Gauss2, including their totals, means, and standard deviations. We can also compute such quantities as Rem(1)+Rem(2) and Rem(18)+Rem(19), which indicate the behavior of the bouncing balls near the sides of the RMC.

Table 3 gives a list of 14 of these quantities, called v1, . . . ,v14, along with their means and standard deviations over our entire set of RMC data, which consists of 4530 (=3×1510) runs. Table 4 (p. 12) lists the correlation coefficients for pairs of the variables v1, . . . ,v14. These are also computed using the entire data set.

We wanted to study a set of bin distribution variables that have as little statistical correlation as possible, but are also physically meaningful. One way of doing this is to eliminate strongly correlated variables from the set v1, . . . ,v14 until a set of nearly

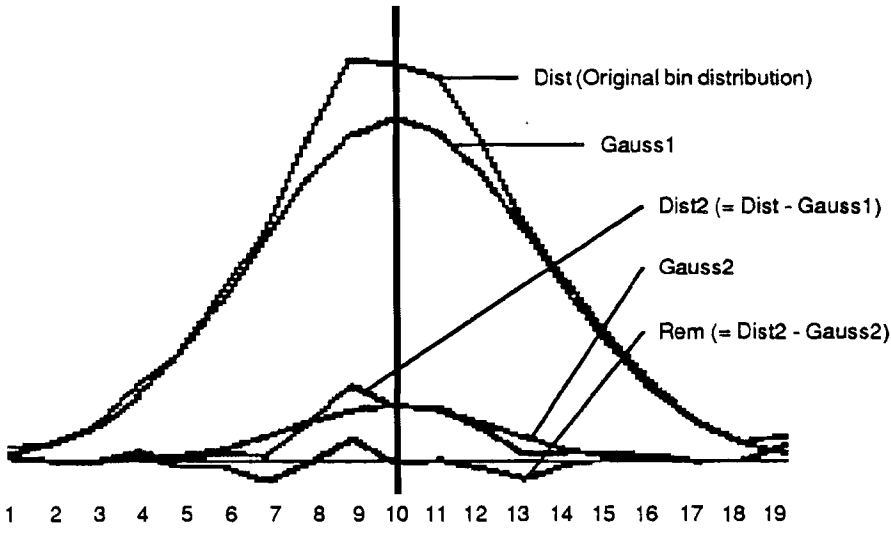

Figure 2(a). Breakdown of bin distribution into component curves.

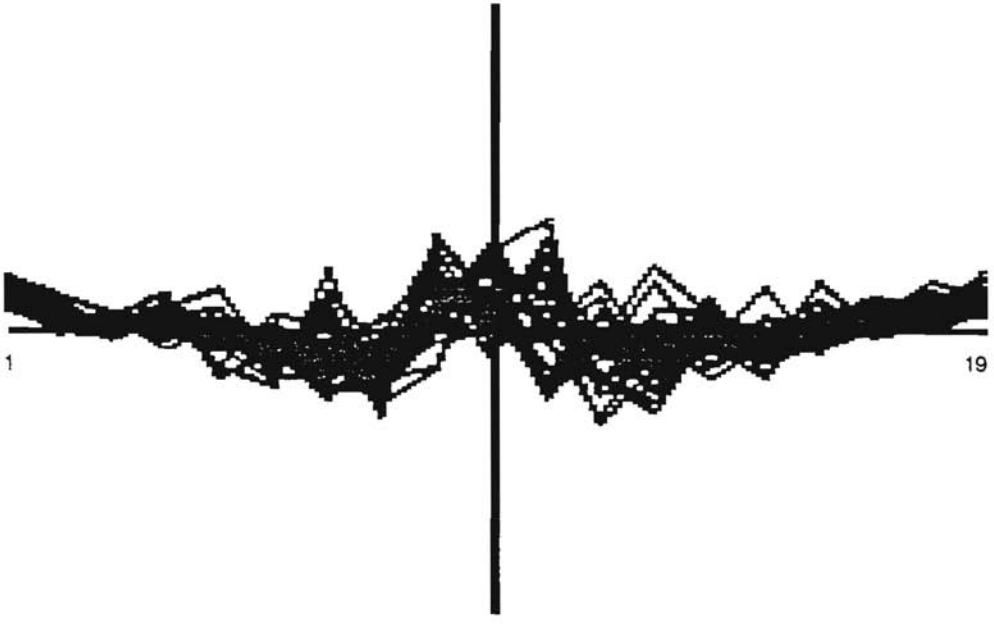

Figure 2(b). Superposition of 30 examples of Rem (= Dist - Gauss1 - Gauss2).

TABLE 3

A Set of 14 Bin Distribution Variables, Based on Gauss1, Gauss2, and Rem

Vble.	Mean	S.D.	Description
v1	10.00815	.2449407	Mean of Dist-Gauss1
v2	10.03411	.07741240	Mean of Dist restricted to bins 3–7,13–17
v3	115.9227	11.83476	Dist(18)+Dist(19)
v4	10.01776	.03823768	Mean of Dist
v5	10.01936	.05283375	Mean of Gauss1
v6	10.04796	.2120386	Mean of Gauss2
v7	3.274984	.03832880	S.D. of Dist
v8	38.30024	12.21952	Rem(18)+Rem(19)
v9	3.305223	.0684025	S.D. of Gauss1
v10	2.670611	.2378355	S.D. of Gauss2
v11	7774.604	443.9916	Total of Gauss1
v12	1157.425	447.0527	Total of Gauss2
v13	67.96227	27.94378	Total of Rem
v14	42.35798	12.34411	Rem(1)+Rem(2)

TABLE 4

Statistical Correlations over the Total Data Set for Variables v1, . . . ,v14

	2	3	4	5	6	7	8	9	10	11	12	13	14
1	-.11	.29	.18	-.46	.85	-.04	.38	-.02	-.01	-.04	.04	.01	-.33
2		.05	.89	.85	.00	-.08	-.13	-.01	-.09	-.01	.02	-.04	.18
3			.28	.03	.01	.53	.82	.22	-.11	.04	-.06	.27	.05
4				.74	.12	-.10	.12	-.03	-.08	-.04	.04	-.04	-.08
5					-.42	-.07	-.17	-.01	-.07	.00	.00	-.05	.17
6						.00	.08	-.04	.00	.03	-.03	.02	.00
7							.10	.59	.12	.04	-.05	.16	.17
8								-.28	.05	.09	-.12	.52	.14
9									-.41	-.45	.48	-.55	-.26
10										.03	-.08	.68	.03
11											-1.00	.09	.18
12												-.15	-.21
13													.49

The total data set contains 4530 bin distributions.

uncorrelated variables remains. Table 5 shows the result of doing this.

In the set of variables of Table 5, v4 is the bin mean, which the RMC operators tried to directly influence. The other 6 variables were presumably not the object of operator or experimenter intentions, and they would be hard for the operator to recognize by observing the machine. Our question is: Do these other variables display behavior significantly correlated with operator intention? A selection theory would imply they should not do this, but it turns out that some of them do.

In Table 6 (p. 14) we list results of an analysis similar to that reported in Tables I.A–C in Nelson *et. al.* (1988a). For this purpose, we made use of the total data set of 1510 tripolar sets of runs that was available to us.

For each tripolar set of runs, the differences v4(i,LT)-v4(i,BL), v4(i,RT)-v4(i,BL), and v4(i,RT)-v4(i,LT) were computed, where v4(i,LT), v4(i,BL), and v4(i,RT) are the bin means obtained under leftward, baseline, and rightward intentions for the ith tripolar set. (Here i=1, . . . ,1510.) The means and standard deviations for these three differences were computed for the 1510 cases, and were used to compute corresponding Student t-scores and probabilities. The probabilities indicate how likely it is that the means of the differences would be displaced by chance from 0 to their observed values. The main point made by Jahn and his colleagues is that these probabilities turn out to be unexpectedly low.

We performed the same computations for each of the remaining 6 variables of Table 5, plus the additional variable, v5. For example, for variable v14 the computations were done for the differences, v14(i,LT)-v14(i,BL), v14(i,RT)-v14(i,BL), and v14(i,RT)-v14(i,LT).

TABLE 5

A Subset of the Variables v1, . . . ,v14
Which are Nearly Statistically Independent of One Another

		6	7	8	10	11	14
4	Mean of Dist	.12	-.10	.12	-.08	-.04	-.08
6	Mean of Gauss		.00	.08	.00	.03	.00
7	S.D. of Dist			.10	.12	.04	.17
8	Rem(18)+Rem(19)				.05	.09	.14
10	S.D. of Gauss2					.03	.03
11	Total of Gauss1						.18
14	Rem(1)+Rem(2)						

Table 6 (p. 14) enables us to compare the probabilities computed for each of these 7 variables (namely, v5, v6, v7, v8, v10, v11, and v14) with the probabilities computed for the bin mean, v4. In the table, the three differences are indicated for each variable by the symbols LT-BL (left minus baseline), RT-BL (right minus baseline), and RT-LT (right minus left). The t-scores are written with a minus sign if the corresponding quantity had a negative displacement. Also indicated are the correlation coefficients between the difference pairs for each of the 7 variables and the difference pairs for v4.

It is natural for the displacement probabilities for variables v4 and v5 to be similar, since these variables have a correlation of about .71 for each of the three differences. Thus v4 has probabilities of .00026 and .000011 for LT-BL and RT-LT, and v5 has similar probabilities for these differences. These small probabilities represent the main anomalous effect. However, if we look at variables v6, v7, v8, v10, v11, and v14, we can see that they also tend to have moderately low probabilities for LT-BL and RT-LT, even though they have very small correlations with v4.

One might ask whether or not this might be statistically significant. The answer is that, individually, the displacements of these variables are not highly significant, but they are highly significant when taken together as a group. Since the variables tend to be mutually uncorrelated, this can be shown by summing them up and examining the displacement of the sum.

With this aim in mind, the calculations of Table 6 were also performed for two composite variables:

$$v15 = Z(v6)+Z(v7)+Z(v8)-Z(v10)-Z(v11)+Z(v14) \quad (8)$$

and

$$v16 = Z(v6)+Z(v7)+Z(v8)+Z(v14) \quad (9)$$

TABLE 6

Comparison Between the Behavior of the Bin Mean, v4, and Variables v5, v6, v7, v8, v10, v11, v14, v15, and v16 for the Total Data Set of 1510 Tripolar Runs

Vble	Intent	Mean	S.D.	T-score	Prob.	Correlation
4	LT-BL	-.00442	.04954	-3.4708	.26e-03	
4	RT-BL	.00093	.05027	.7226	.23e+00	
4	RT-LT	.00536	.04900	4.2505	.11e-04	
5	LT-BL	-.00651	.07133	-3.5440	.20e-03	.71224
5	RT-BL	.00060	.06940	.3338	.37e+00	.71254
5	RT-LT	.00710	.06899	3.9998	.32e-04	.71093
6	LT-BL	.01204	.30035	1.5576	.60e-01	.08837
6	RT-BL	.00925	.30459	1.1802	.12e+00	.14267
6	RT-LT	-.00279	.29772	-.36409	.36e+00	.11919
7	LT-BL	.00182	.03513	2.0090	.22e-01	-.02635
7	RT-BL	.00017	.03619	.1820	.43e+00	-.03020
7	RT-LT	-.00165	.03619	-1.7681	.39e-01	.01406
8	LT-BL	.11436	17.26166	.2574	.40e+00	.12766
8	RT-BL	-.85697	17.01353	-1.9573	.25e-01	.09323
8	RT-LT	-.97133	16.79172	-2.2478	.12e-01	.10980
10	LT-BL	-.00687	.30911	-.8634	.19e+00	.00251
10	RT-BL	-.01479	.31592	-1.8195	.34e-01	.00838
10	RT-LT	-.00792	.31020	-.9926	.16e+00	-.01635
11	LT-BL	-8.18748	619.03754	-.5140	.30e+00	.00147
11	RT-BL	2.16578	627.71466	.1341	.45e+00	.00052
11	RT-LT	10.35326	622.28522	.6465	.26e+00	.02146
14	LT-BL	.36884	16.46020	.8708	.19e+00	-.09009
14	RT-BL	-.44194	17.14941	-1.0014	.16e+00	-.12368
14	RT-LT	-.81078	17.46187	-1.8043	.36e-01	-.08725
15	LT-BL	.19072	3.07315	2.4116	.79e-02	.05073
15	RT-BL	-.00057	3.12211	-.0071	.50e+00	.03925
15	RT-LT	-.19129	3.09071	-2.4050	.81e-02	.06450
16	LT-BL	.14340	2.82344	1.9736	.24e-01	.05710
16	RT-BL	-.05788	2.87465	-.7825	.22e+00	.04676
16	RT-LT	-.20129	2.89220	-2.7044	.34e-02	.07195

where Z(variable) is that variable shifted so as to have mean 0 and scaled so as to have a standard deviation of 1 over the 1510 tripolar sets. The transformation Z was applied so as to make the magnitudes of the variables comparable, and thereby prevent the high magnitude variables in the sum from overshadowing the contributions of the low magnitude variables. In v15 the variables v10 and v11 were given a minus sign due to the fact that they vary in a direction opposite to that of variables v6, v7, v8, and v14. (This can be seen by examining Table 6.)

The same computations were performed for v15 and v16 that were performed for v4, v5, v6, v7, v8, v10, v11, and v14, and the results are listed in Table 6. These results indicate that the mild effects noted for the constituent variables of v15 and v16 do seem to add up. We see from the table that v15 has probabilities of .0079 and .0081 for LT-BL and RT-LT, and v16 has corresponding probabilities of .024 and .0034. These probabilities indicate that the group behavior of the variables making up v15 and v16 is significantly different from what would be expected by chance.

Table I.A–C of Nelson *et. al.* (1988a) was computed for a 1131 run subset of the total data set, generated by 25 out of the 35 operators. These comprise all the runs in the total data set in which a single operator observed the RMC machine in operation, in the same room. (Other runs involved multiple operators, or an operator trying to influence the machine at a remote location or at a time before or after the time of the run.) We also performed the calculations of Table 6 for this subset. The results are given in Table 7 (p. 16).

In Table 7 we see that v15 has probabilities of .00015 and .00075 for LT-BL and RT-LT, and v16 has probabilities of .00057 and .00034. These are roughly an order of magnitude higher than the corresponding probabilities for v4 in Table 7, but they are certainly significant. In general, one tends to obtain lower probabilities for the 1131 case subset than for the full data set of 1510 cases. What is happening here is that anomalous effects are much weaker in the part of the data set involving either multiple operators or operators who could not see the RMC in operation.

We note that the correlation coefficient of v4 and v15 is .073 (over the entire data set), and that of v4 and v16 is .028. The correlation coefficients between the difference pairs for v15 and v16 and the corresponding difference pairs for v4 are listed in Table 7, and also lie between 0 and .1. (Recall that the difference pairs are v15(i,LT)-v15(i,BL), and so on.) Thus the improbable displacements of v15 and v16 cannot be accounted for by the hypothesis that v15 and v16 shift in correlation with the shift in v4. In fact, the displacements of v15 and v16 for LT-BL and RT-LT go in the direction opposite to the corresponding displacements of v4. These displacements constitute an anomalous effect that is independent of the original anomalous effect reported by Jahn and his colleagues. Moreover, this effect is due to the behavior of variables (the constituents of v15 and v16) which could not be observed by the operators, and were not the objects of operator intentions.

If we examine the 4530 pairs, (v4,v15), we find that their distribution can be approximated by a bivariate normal distribution. The same is true of the pairs, (v4,v16). This means that Eqn. (5) should apply with v=v4 and u=v15 or v16. This equation implies, for example, that

$$[E(v15|LT)-E(v15|BL)]/s_{v15} = r[E(v4|LT)-E(v4|BL)]/s_{v4} \qquad (10)$$

TABLE 7

Comparison Between the Behavior of the Bin Mean, v4, and Variables v5, v6, v7, v8, v10, v11, v14, v15, and v16 for 1131 Runs Generated by 25 Operators

Vble	Intent	Mean	S.D.	T-score	Prob.	Correlation
4	LT-BL	-.00564	.05005	-3.7870	.76e-04	
4	RT-BL	.00007	.05008	.0472	.48e+00	
4	RT-LT	.00571	.04931	3.8913	.50e-04	
5	LT-BL	-.00789	.07090	-3.7420	.91e-04	.70955
5	RT-BL	.00001	.06938	.0065	.50e+00	.72223
5	RT-LT	.00790	.06927	3.8364	.62e-04	.71710
6	LT-BL	.01124	.29531	1.2799	.10e+00	.09233
6	RT-BL	.00373	.29996	.4178	.34e+00	.12404
6	RT-LT	-.00751	.29278	-.8629	.19e+00	.12407
7	LT-BL	.00321	.03500	3.0875	.10e-02	-.04128
7	RT-BL	.00085	.03578	.8003	.21e+00	-.03315
7	RT-LT	-.00236	.03630	-2.1881	.14e-01	.01918
8	LT-BL	.70664	17.63451	1.3476	.89e-01	.16174
8	RT-BL	-.59116	17.25134	-1.1524	.12e+00	.08853
8	RT-LT	-1.29780	16.99774	-2.5677	.51e-02	.12033
10	LT-BL	-.00397	.30761	-.4343	.33e+00	.00937
10	RT-BL	-.01122	.31699	-1.1900	.12e+00	.02250
10	RT-LT	-.00724	.31543	-.7724	.22e+00	-.00912
11	LT-BL	-18.69107	630.79480	-.9965	.16e+00	.01230
11	RT-BL	-4.65074	632.71381	-.2472	.40e+00	.00503
11	RT-LT	14.03979	627.16571	1 .7529	.23e+00	.03185
14	LT-BL	1.02498	16.41335	2.1001	.18e-01	-.10295
14	RT-BL	-.10467	16.80345	-.2095	.42e+00	-.10887
14	RT-LT	-1.12965	17.39774	2.1836	.14e-01	-.07294
15	LT-BL	.33160	3.08571	3.6140	.15e-03	.05171
15	RT-BL	.03976	3.08411	.4336	.33e+00	.02832
15	RT-LT	-.29184	3.08992	-3.1764	.75e-03	.07167
16	LT-BL	.27337	2.82734	3.2517	.57e-03	.06682
16	RT-BL	-.01755	2.87298	-.2055	.42e+00	.04326
16	RT-LT	-.29093	2.88306	-3.3936	.34e-03	.08805

where r lies between 0 and .1. But this is contradicted by the actual behavior of v15, which shifts strongly in the positive direction in this case, even though v4 shifts strongly in the negative direction.

In addition to the calculations presented in Table 7, we produced graphs showing the behavior of the 10 variables, v4, . . . ,v16. For these graphs we adopted the following procedure. First, the variables were all scaled so as to have mean 0 and standard deviation 1. That is, we replaced vk by Z(vk) for each of the variables. We then formed all of the pairs, (v4,vk), for k=5,6,7,8,10,11,14,15,16. For the pair, (v4,vk), define the two dimensional random variable (X_{2n-1},Y_{2n-1}) to be (v4,vk), computed for the nth tripolar set with leftward intention. Similarly, define (X_{2n},Y_{2n}) to be (-v4,-vk), computed for the nth tripolar set with baseline intention. We plotted the random walk generated by steps of (X_n,Y_n) for n=1, . . . ,2×1510.

We will let (S_n,T_n) represent the random walk generated by steps of (X_n,Y_n). Thus, $S_0=T_0=0$ and

$$(S_n,T_n) = (X_n,Y_n) + (S_{n-1},T_{n-1}) \tag{11}$$

For each tripolar set of runs, this random walk takes one step of (v4,vk) for the run of intention, LT, and one oppositely directed step of (-v4,-vk) for the run of intention, BL. This gives us an idea of the comparative behavior of v4 and vk in the case LT-BL. Similar random walks were plotted for the cases RT-BL and RT-LT. We also plotted these random walks for the subset of 1131 tripolar sets in which a single operator was watching the RMC, for the subset of tripolar sets generated by operator 10, and also for the subset in which operator 10 was watching the RMC.

For a given angle, Θ, the random walk can be projected onto the line through the origin at angle Θ. This projected random walk is

$$U_n = \cos(\Theta)S_n+\sin(\Theta)T_n \tag{12}$$

The standard deviation of U_n is $[n(1+\sin(2\Theta)r)]^{.5}$, where r is the correlation coefficient for X_n and Y_n. If we assume that v4 and vk keep the same statistical properties for tripolar sets in the interval from n=1 to 2×1510, and that operator intention is irrelevant to their behavior, then r is the correlation coefficient between v4 and vk, as estimated in Table 5 (p. 13). (This table should be supplemented with values for r of .073, .028, .814 for (v4,v15), (v4,v16), and (v15,v16), respectively.) Although there is some change in the statistical properties of the vk's with the passage of time (represented by n), the curve,

$$R = 2[N(1+\sin(2\Theta)r)]^{.5} \tag{13}$$

provides a two standard deviation limit that can be used to evaluate the behavior of (S_n,T_n) for n=1, . . . ,N.

Figures 3(a–f) through 7(a–f) (pp. 18–22) show some of the plots of these random walks, along with their estimated two standard deviation limits. In each graph, S_n is plotted along the x-axis and T_n is plotted on the y-axis. Graphs (a), (c), and (e) are for the subset of the 1510 tripolar sets generated by operator 10, who was the most successful operator in

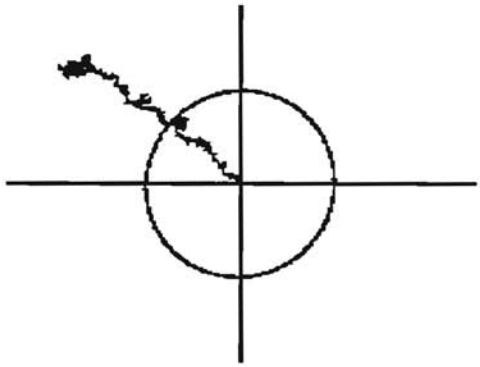

Figure 3(a). Operator 10, left-baseline. Parameters (4,16) are the (x,y) axes.

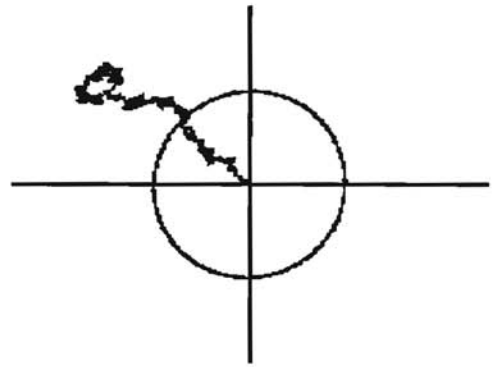

Figure 3(b). All operators, left-baseline. Parameters (4,16) are the (x,y) axes.

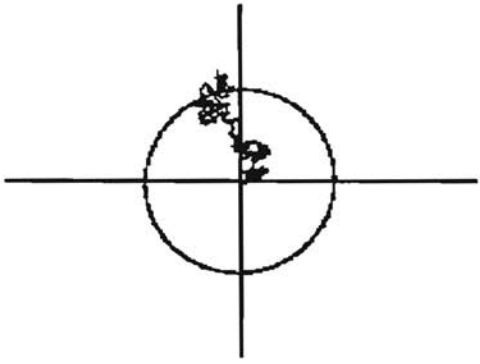

Figure 3(c). Operator 10, right-baseline. Parameters (4,16) are the (x,y) axes.

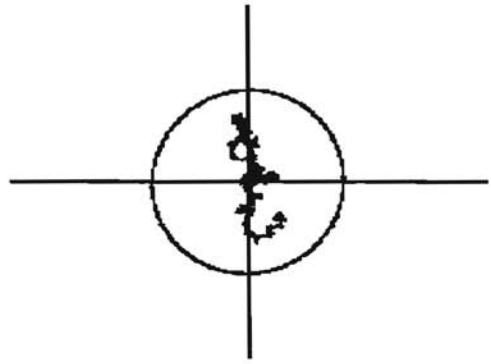

Figure 3(d). All operators, right-baseline. Parameters (4,16) are the (x,y) axes.

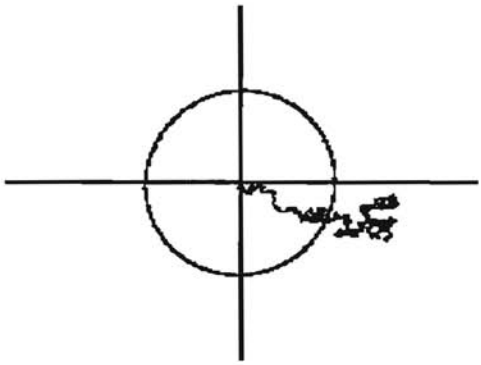

Figure 3(e). Operator 10, right-left. Parameters (4,16) are the (x,y) axes.

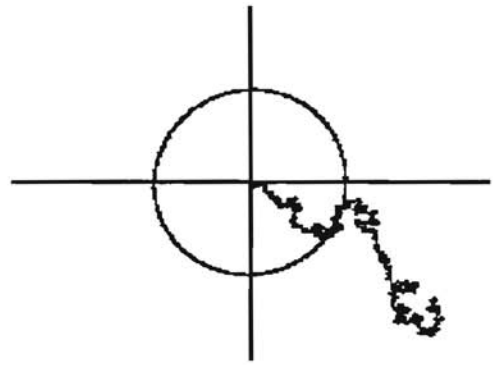

Figure 3(f). All operators, right-left. Parameters (4,16) are the (x,y) axes.

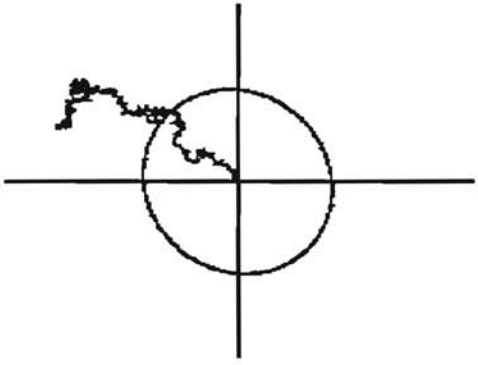

Figure 4(a). Operator 10, left-baseline. Parameters (4,14) are the (x,y) axes.

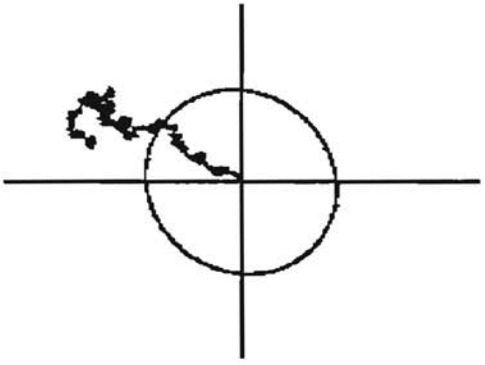

Figure 4(b). All operators, left-baseline. Parameters (4,14) are the (x,y) axes.

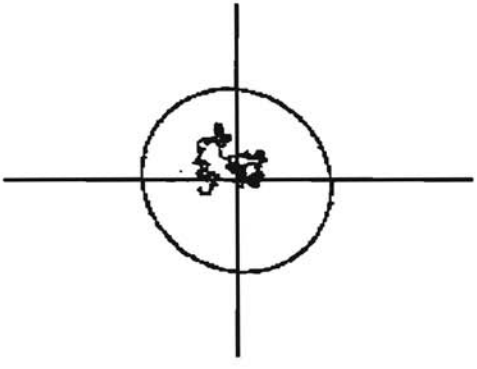

Figure 4(c). Operator 10, right-baseline. Parameters (4,14) are the (x,y) axes.

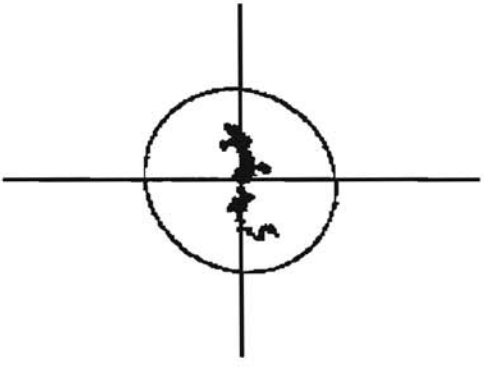

Figure 4(d). All operators, right-baseline. Parameters (4,14) are the (x,y) axes.

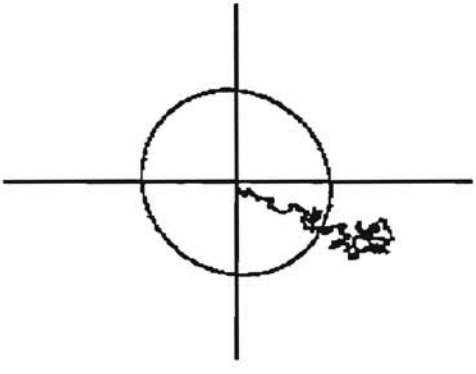

Figure 4(e). Operator 10, right-left. Parameters (4,14) are the (x,y) axes.

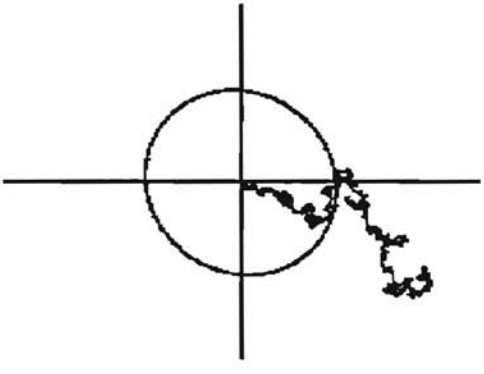

Figure 4(f). All operators, right-left. Parameters (4,14) are the (x,y) axes.

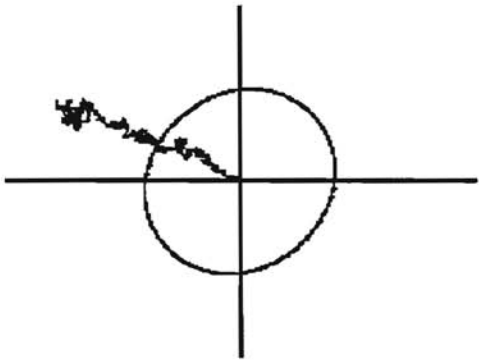

Figure 5(a). Operator 10, left-baseline. Parameters (4,8) are the (x,y) axes.

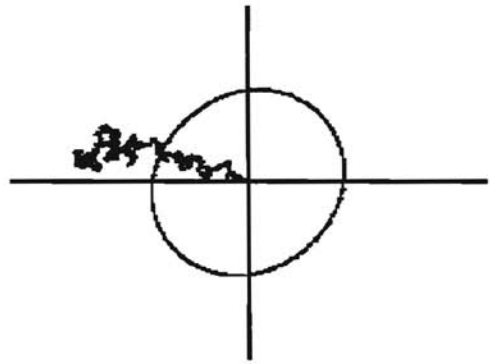

Figure 5(b). All operators, left-baseline. Parameters (4,8) are the (x,y) axes.

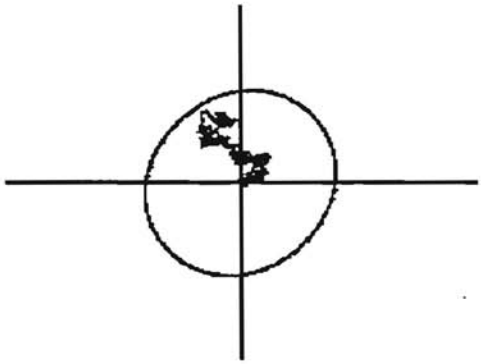

Figure 5(c). Operator 10, right-baseline. Parameters (4,8) are the (x,y) axes.

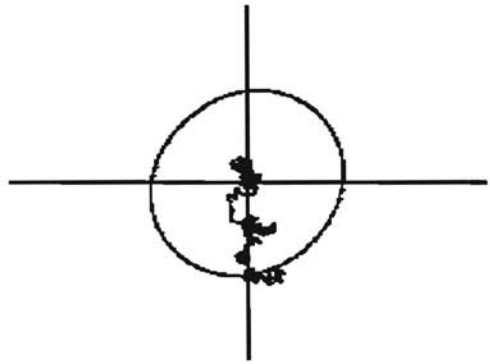

Figure 5(d). All operators, right-baseline. Parameters (4,8) are the (x,y) axes.

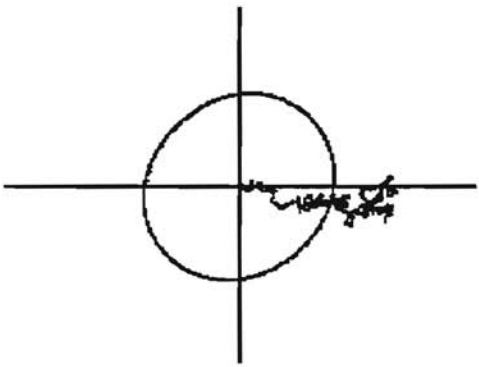

Figure 5(e). Operator 10, right-left. Parameters (4,8) are the (x,y) axes.

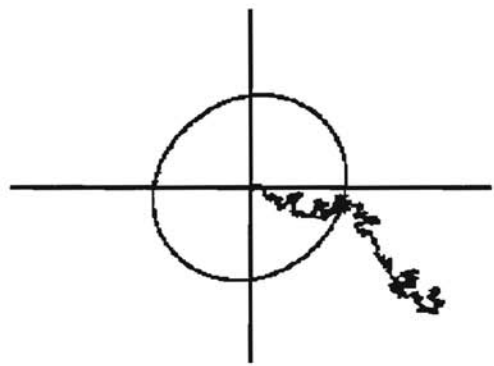

Figure 5(f). All operators, right-left. Parameters (4,8) are the (x,y) axes.

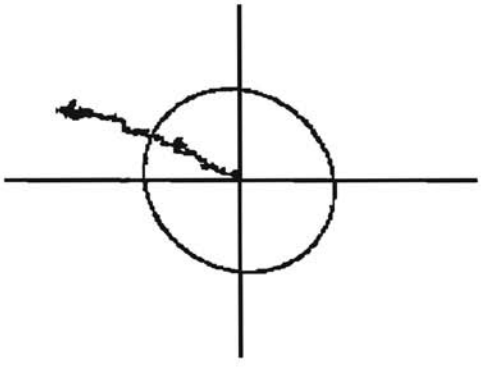

Figure 6(a). Operator 10, left-baseline. Parameters (4,7) are the (x,y) axes.

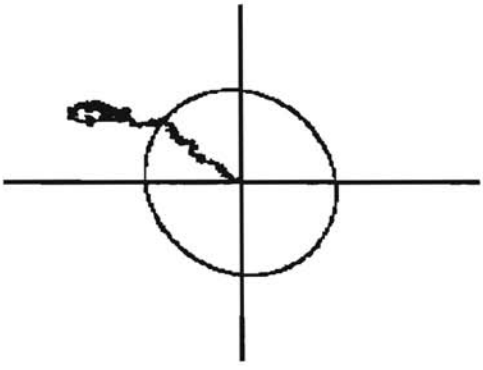

Figure 6(b). All operators, left-baseline. Parameters (4,7) are the (x,y) axes.

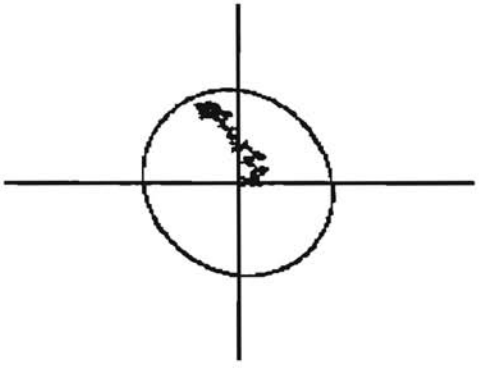

Figure 6(c). Operator 10, right-baseline. Parameters (4,7) are the (x,y) axes.

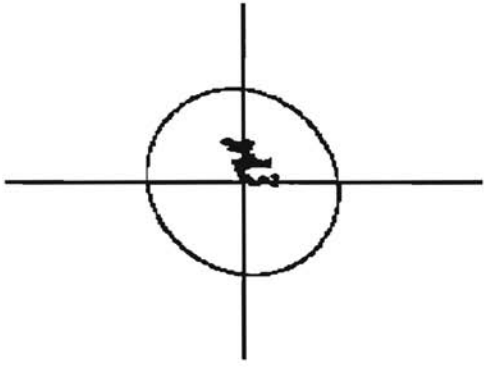

Figure 6(d). All operators, right-baseline. Parameters (4,7) are the (x,y) axes.

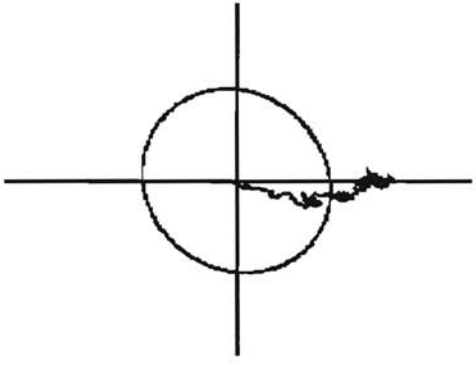

Figure 6(e). Operator 10, right-left. Parameters (4,7) are the (x,y) axes.

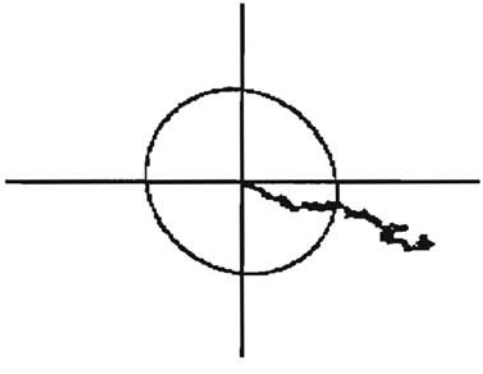

Figure 6(f). All operators, right-left. Parameters (4,7) are the (x,y) axes.

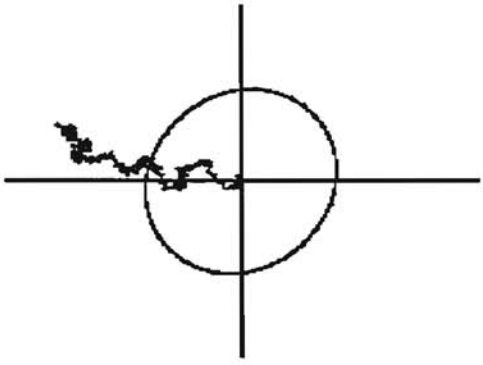

Figure 7(a). Operator 10, left-baseline. Parameters (4,6) are the (x,y) axes.

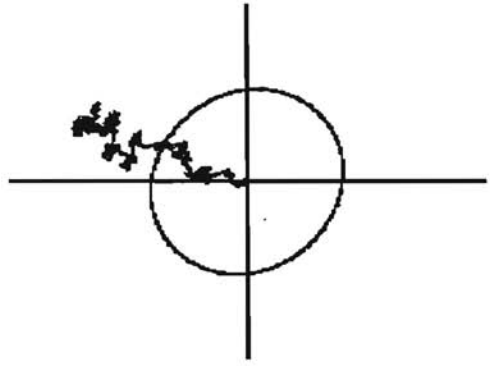

Figure 7(b). All operators, left-baseline. Parameters (4,6) are the (x,y) axes.

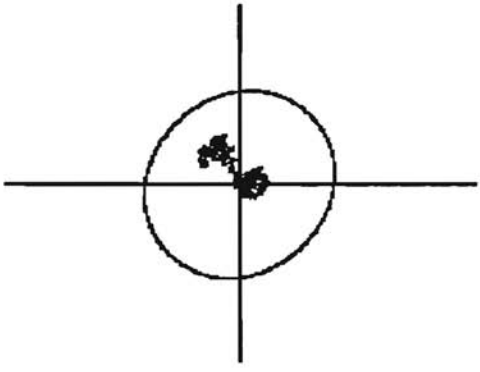

Figure 7(c). Operator 10, right-baseline. Parameters (4,6) are the (x,y) axes.

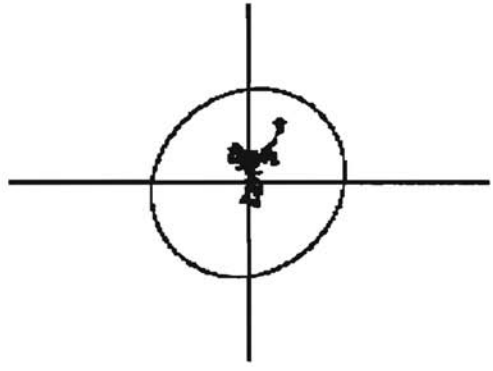

Figure 7(d). All operators, right-baseline. Parameters (4,6) are the (x,y) axes.

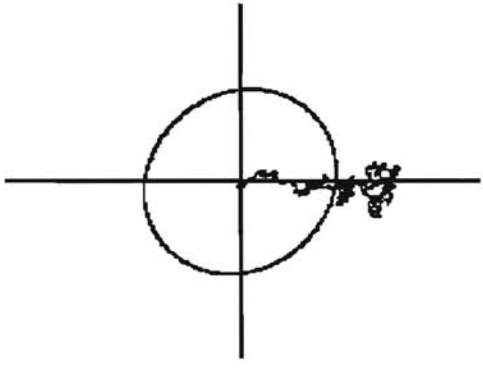

Figure 7(e). Operator 10, right-left. Parameters (4,6) are the (x,y) axes.

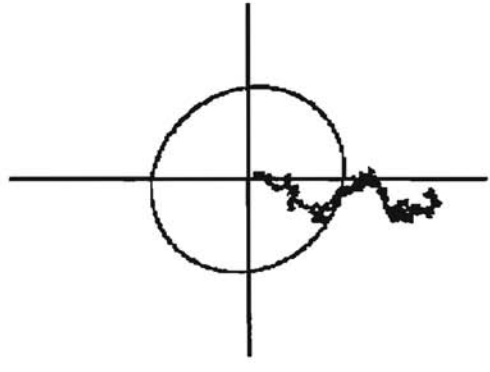

Figure 7(f). All operators, right-left. Parameters (4,6) are the (x,y) axes.

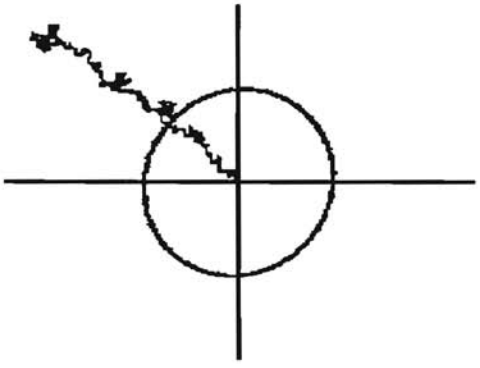

Figure 8(a). Operator 10, left-baseline. Parameters (4,16) are the (x,y) axes. Case of 1131 runs.

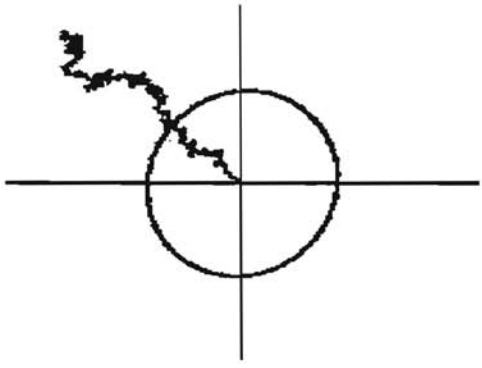

Figure 8(b). All operators, left-baseline. Parameters (4,16) are the (x,y) axes. Case of 1131 runs.

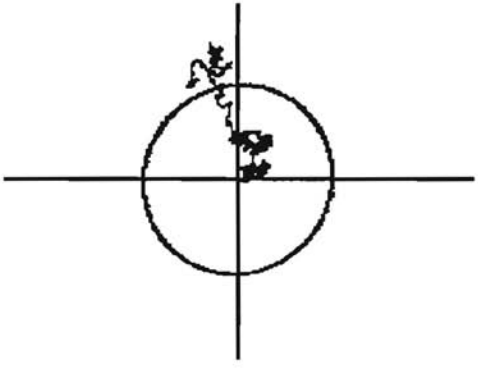

Figure 8(c). Operator 10, right-baseline. Parameters (4,16) are the (x,y) axes. Case of 1131 runs.

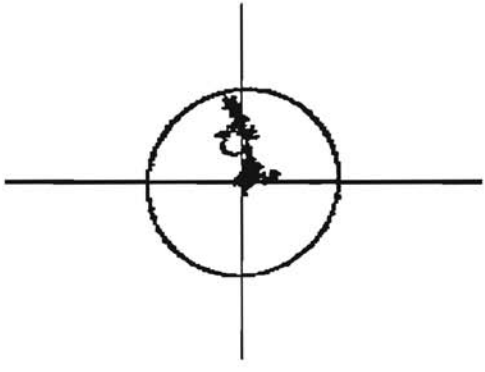

Figure 8(d). All operators, right-baseline. Parameters (4,16) are the (x,y) axes. Case of 1131 runs.

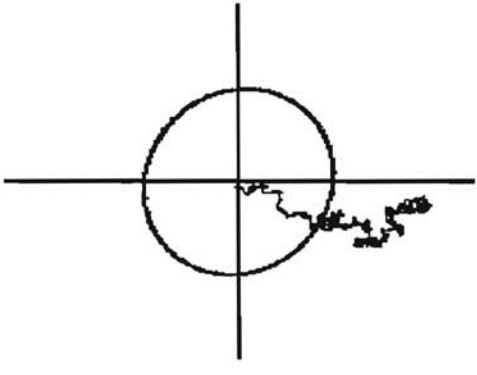

Figure 8(e). Operator 10, right-left. Parameters (4,16) are the (x,y) axes. Case of 1131 runs.

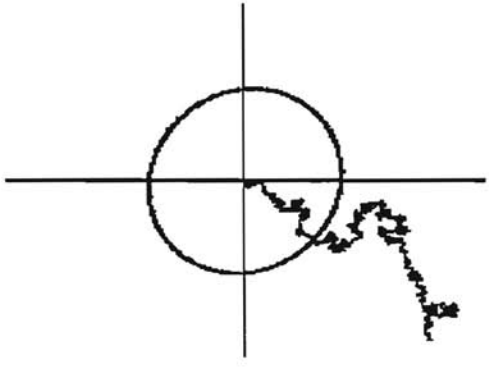

Figure 8(f). All operators, right-left. Parameters (4,16) are the (x,y) axes. Case of 1131 runs.

Figure 9. Superposition of 100 RMC random walks with randomized intention. Parameters (4,16) are the (x,y) axes.

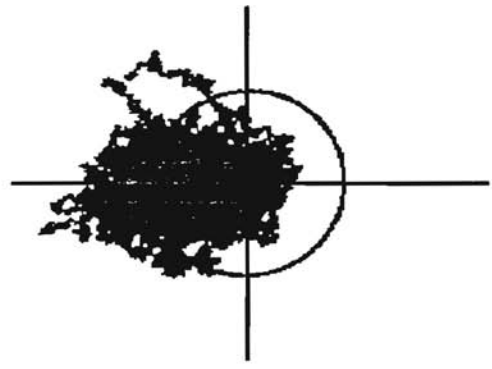

Figure 10. Superposition of 100 RMC random walks with randomized intention and artificial selection of parameter 4 low (i.e. to the left). Parameters (4,16) are the (x,y) axes.

the RMC experiments. Graphs (b), (d), and (f) are for all 1510 tripolar runs and include all operators. In Figures 8(a–f) (p. 23) we show similar plots of the random walks for the subset of 1131 tripolar sets in which a single operator watched the RMC in operation.

We can see in these figures the basic anomaly revealed by the RMC experiments. Since S_n, representing the bin mean, is plotted on the x-axis, this takes the form of a shift of the random walk to the left in the LT-BL cases, and to the right in the RT-LT cases. Oddly enough, there is very little displacement to the right or left in the case of RT-BL.

The graphs also show an additional tendency for the other variables, especially v15 and v16, to drift systematically away from the origin, rather than moving back and forth in the manner of a random walk. It is interesting to note that the systematic drift of (S_n,T_n) is in many cases perpendicular to the direction of correlation between X_n and Y_n. (This direction is indicated by the bulge of the two standard deviation curve.) In addition, we note that Figures 3(c)–8(c) and 3(d)–8(d) (pp. 18–23) show a pronounced anomalous displacement of v16, v14, v8, and v7 in the case of RT-BL, even though v4 does not show much displacement in this case. This displacement is in the same direction as the displacement of these variables in the LT-BL case, and therefore the RT-LT displacement tends to be reduced (since RT-LT = RT-BL - LT-BL).

Our general comment concerning these random walk graphs is that they seem to show many highly non-random features. In particular, this is true of Figure 8(a) (p. 23), where the random walk practically follows a straight line.

To test whether or not this apparent nonrandomness is illusory, we performed a number of probabilistic experiments using the RMC data. The results of the first of these experiments are summed up in Figure 9. There we have superimposed 100 random walks which are generated in nearly the same way as the random walks in Figures 3(b,d,f) (p. 18), the case of v4 vs. v16 for all operators. The only difference is that in each tripolar set, the +(v4,v16) and -(v4,v16) steps of the random walk are chosen at random from the three runs in that set, instead of being chosen on the basis of intention. The random choices were made using a psuedo-random number generator. The idea here is to create random walks that are

identical to the random walks of Figures 3(b,d,f) (p. 18) with the exception that information concerning operator intentions is erased by random scrambling. Figure 9 shows that these random walks show no particular tendency for systematic drift, apart from a slight tilt with positive slope which may be due to the small positive correlation between v4 and v16. Thus, all of the anomalous effects in Figures 3(b,d,f) seem to depend on the information regarding operator intentions.

The results of the second experiment are shown in Figure 10. This experiment is the same as the first, with one exception: In the random walks, if a step is positive in v4, then it is rejected with a certain probability; if it is negative then it is always accepted. This rule has the effect of imposing an artificial bias against movement in the positive v4 direction (the positive x-axis in the plots). This is exactly the kind of bias we would postulate in the "data selection" theory described in the previous section. If that theory is correct, then these random walks should be similar to the one plotted in Figure 3(b).

We can see from Figure 10 that, with a couple of exceptions, there is no tendency for the random walks generated in this way to mimic Figure 3(b), the real random walk for variables v4 and v16 and intentions LT-BL. The artificially generated random walks do show a tendency to drift systematically to the left, but instead of also drifting in the positive y direction, they exhibit, if anything, the opposite tendency.

We also considered the following hypothesis: Suppose there is a variable, w, that is weakly correlated with both v4 and v16. Perhaps the joint displacements of v4 and v16 can be explained as a result of selection applied to w. To investigate this hypothesis properly, one would have to consider many different candidates for w. We investigated only two possible w's, and neither one could account for the observed displacements of v4 and v16.

4. CONCLUSION

The basic conclusion that emerges from this study is that in addition to the original anomalies reported by Jahn and his colleagues, the statistical behavior of the bin distributions seems to display systematic patterns that correlate with human intentions, but are not related in an obvious way to the conscious content of those intentions. Thus, the data show a systematic shift in v4, the bin mean, but they also show shifts in v15, and v16. These, in turn, are due to the summing up of shifts in the constituent variables of v15 and v16, namely v6, v7, v8, v10, v11, and v14. The shifts in v15 and v16 are somewhat less improbable than the shift in the bin mean, but they are nonetheless statistically significant. This is especially true for the set of 1131 runs in which a single operator was present during the running of the RMC (Table 7, p. 16).

The shifts in v15, v16, and their constituent variables cannot be accounted for by inter-variable correlations with the bin mean that could be due to the physical characteristics of the RMC device. The reason for this is that we can calculate the correlations between v4 and other vk's over the whole data set, without taking operator intentions into account. When this is done, it is found that the resulting correlations are too small to account for the observed shifts in the different variables, and in some cases, including v15 and v16, these correlations tend in the wrong direction.

These findings tend to rule out a class of theories, called selection theories, which might be invoked to explain the anomalies in the RMC data. In particular, they tend to rule out the possibility that the main anomalous effect in the bin mean was obtained by conscious or subconscious data selection by the experimenters. Certainly a drift in v4 in a given direction can be obtained by systematically throwing out a certain percentage of the runs which do not tend in that direction. However, as we have seen, such editing of the data will not generate the additional shifts that we have observed in certain other variables, and it seems unlikely that these variables could have been the object of additional data selection by the experimenters.

Theoretical calculations suggest that it would be difficult for the operators to generate the observed anomalous effects by exerting small, normal forces on the RMC (of the kind that could be produced by a human body at a distance from the machine). This is not because the RMC is insensitive to such forces, but because it is too sensitive to them. To create a desired shift of the bin mean by exerting some force, one would have to apply the force with great precision. And to determine what amount of force to apply, one would have to take into account the unpredictable influence of many other forces arising within the general environment of the RMC.

What we are left with is the conclusion that some unknown agency affects the behavior of the RMC in accordance with conscious intentions of the operators. This agency not only affects the bin mean, which is the object of the operators' intentions, but it also affects other aspects of RMC behavior which would be expected to vary independently of this variable. To learn more about what is happening here, we would recommend future experiments in which many different aspects of a physical process are monitored, while efforts are being made to influence particular features of that process. Such experiments would reveal whether or not the phenomena we have observed here generally occur, and they may give further insight into the causes of these phenomena.

REFERENCES

R. D. Nelson, B. J. Dunne, & R. G. Jahn (1984), *An REG Experiment with Large Data Base Capability, III: Operator Related Anomalies*, (School of Engineering/Applied Science, Princeton Univ.)

R. D. Nelson, B. J. Dunne, & R. G. Jahn (1988a), *Operator Related Anomalies in a Random Mechanical Cascade Experiment*, (School of Engineering/Applied Science, Princeton Univ.)

R. D. Nelson, B. J. Dunne, & R. G. Jahn (1988b), *Operator Related Anomalies in a Random Mechanical Cascade Experiment, Supplement*, (School of Engineering/Applied Science, Princeton Univ.)

E. P. Wigner, "Physics and the Explanation of Life," *Found. of Phys.* 1, 35 (1970)